LETTER
IEICE Electronics Express, Vol.13, No.19, 1–7

Characterization of the field-dependent permittivity of $Ba_{0.5}Sr_{0.5}TiO_3$ thin films up to 110 GHz

Jingtian Liu[1,2], Shuming Chen[1,2a)], Xi Ning[1,2], Jinying Zhang[3], Lei Wang[1,2], and Zhi Wang[1,2]

[1] *College of Computer, National University of Defense Technology, Changsha 410073, P. R. China*

[2] *National Laboratory for Parallel and Distributed Processing, National University of Defense Technology, Changsha 410073, P. R. China*

[3] *Institute of Semiconductors, Chinese Academy of Sciences, Beijing 100083, P. R. China*

a) *smchen@nudt.edu.cn*

Abstract: Perovskite $Ba_{0.5}Sr_{0.5}TiO_3$ (BST) thin films with a thickness of 300 nm are deposited on high resistivity silicon through pulsed laser deposition. The permittivity of BST is changed by applying an external electrostatic field. Coplanar waveguides (CPWs) are designed to extract the field-dependent permittivity of the film in the frequency range from 1 GHz to 110 GHz. A Subregional Match 3-Dimensional finite element method (SM 3D FEM) is proposed to implement the permittivity extraction. We analysis the electric field distribution in BST film, and thus divide the BST film in a reasonable way in order to achieve the permittivity of each small region in BST film by S-parameters-phase matching. The relative difference between measured and simulated S-parameters-phase is defined to describe the precision of the result. Experimental results show that the relative difference is less than 1.3%. We also found that the permittivity tunability is almost unchanged in a wide frequency domain, the variation of the tunability less than 0.16. The relative dielectric permittivity ξ_{BST} at 0 V equals 1148.9 at 1 GHz and reduces to 311.7 at 110 GHz, and ξ_{BST} at 100 GHz equals 315.8 at 0 V and declines to 193.4 at 30 V. The tunability of BST film is about 38.7% at 100 GHz.

Keywords: characterization, coplanar line, BST, non-uniform film, finite-difference-time-domain (FDTD), permittivity, tunable

Classification: Electron devices, circuits and modules

References

[1] P. M. Suherman, *et al.*: "Microwave properties of $Ba_{0.5}Sr_{0.5}TiO_3$ thin film coplanar phase shifters," J. Appl. Phys. **99** (2006) 104101 (DOI: 10.1063/1.2198933).

[2] J. H. Leach, *et al.*: "Large dielectric tuning and microwave phase shift at low

DOI: 10.1587/elex.13.20160713
Received July 20, 2016
Accepted August 22, 2016
Publicized September 23, 2016
Copyedited October 10, 2016

IEICE Electronics Express, Vol.13, No.19, 1–7

electric field in epitaxial $Ba_{0.5}Sr_{0.5}TiO_3$ on $SrTiO_3$," J. Appl. Phys. **107** (2010) 084511 (DOI: 10.1063/1.3359707).
[3] M. Sazegar, *et al.*: "Compact tunable phase shifters on screen-printed BST for balanced phased arrays," IEEE Trans. Microw. Theory Techn. **59** (2011) 3331 (DOI: 10.1109/TMTT.2011.2171985).
[4] F. Ponchel, *et al.*: "Rigorous extraction tunability of Si-integrated $Ba_{0.3}Sr_{0.7}$-TiO_3 thin film up to 60 GHz," Appl. Phys. Lett. **96** (2010) 252906 (DOI: 10.1063/1.3454772).
[5] W. J. Kim, *et al.*: "Microwave properties of tetragonally distorted $(Ba_{0.5}Sr_{0.5})$-TiO_3 thin films," Appl. Phys. Lett. **76** (2000) 1185 (DOI: 10.1063/1.125977).
[6] X. Ning, *et al.*: "Propagation-constant matching based broadband permittivity extraction from S-parameter," IEICE Electron. Express **12** (2015) 20150463 (DOI: 10.1587/elex.12.20150463).
[7] X. Ning, *et al.*: "Dielectric microwave properties of Si-integrated pulsed laser deposited $(Ba,Sr)TiO_3$ thin films up to 110 GHz," Appl. Phys. Lett. **107** (2015) 052905 (DOI: 10.1063/1.4927537).
[8] F. Ponchel, *et al.*: "Dielectric microwave characterizations of $(Ba,Sr)TiO_3$ film deposited on high resistivity silicon substrate: Analysis by two-dimensional tangential finite element method," Appl. Phys. Lett. **107** (2010) 054112 (DOI: 10.1063/1.3309423).
[9] A. Giere, *et al.*: "Optimization of uniplanar multilayer structures using nonlinear tunable dielectrics," European Microwave Conference (2005) 1 (DOI: 10.1109/EUMC.2005.1608918).
[10] A. Giere, *et al.*: "Characterization of the field-dependent permittivity of nonlinear ferroelectric films using tunable coplanar lines," IEEE Microw. Wireless Compon. Lett. **17** (2007) 442 (DOI: 10.1109/LMWC.2007.897795).

1 Introduction

$(Ba,Sr)TiO_3$ (BST) thin films exhibit promising dielectric tunable properties in high frequency domain [1, 2], leading to great potential for application in microwave filters and tunable phase shifters [3]. CPW transmission line is commonly used in the extraction of BST thin films characteristic, i.e. permittivity. There are many methods based on CPW transmission line have been proposed, such as CM and quasi-TEM analysis [4, 5] and fast 3D FEM simulation [6, 7] (another work in our group). But these methods assume that the permittivity of the BST film is uniform, not suitable for extraction of non-uniform film properties under an applied electric field. There are also methods focus on non-uniform film properties, such as 2D FEM method [8, 9]. However, wave will not be a pure TEM type at different frequencies due to the losses in the strips.

In this paper, a new extraction method is proposed, called Subregional Match 3-Dimensional finite element method (SM 3D FEM). First S-parameters-phase is calculated from the microwave measurement, and 2-dimensional electrostatic field analysis is applied to calculate the electric field strength distribution to determine the value of the distribution permittivity of BST thin film. Then, BST thin film is solved analytically in each division region by matching the S-parameters-phase, i.e., narrowing the difference between measured and simulated S-parameters phase by adjusting the changeable permittivity in the SM 3D FEM model.

DOI: 10.1587/elex.13.20160713
Received July 20, 2016
Accepted August 22, 2016
Publicized September 23, 2016
Copyedited October 10, 2016

IEICE Electronics Express, Vol.13, No.19, 1–7

Through experiments, methods to extract permittivity from above references and SM 3D FEM are compared in terms of result accuracy and time consumption. We use the relative difference between measured and simulated S-parameters-phase to describe the result accuracy and the number of iterations to characterize the time consumption. Experiments results are described in Table I. In all methods above, SM 3D FEM has the highest accuracy while not have too much time overhead.

Table I. Comparison between different methods of result accuracy and time consumption.

Method	Results accuracy	Time consumption
SM 3D FEM	1.3%	30–50
CM and quasi-TEM analysis	13.5%	1
fast 3D FEM simulation	5.7%	5–6
2D FEM	4.3%	25–30

Coplanar waveguide (CPW) transmission line structure show in Fig. 1. It consist of an high resistivity silicon (hrSi) carrier substrate with a $Ba_{0.5}Sr_{0.5}TiO_3$ film and metal electrodes on top, which encompass a tunable coplanar waveguide (CPW) as a basic element for tunable RF components. The center conductor width S, slot width G, and ground width W, as shown in Fig. 1, are 30 um, 2 um, and 190 um, respectively. The thickness of electrodes t, BST film h_2, and substrate h_1 are 130 nm, 300 nm, and 500 um, respectively. And the CPWs were fabricated with lengths of 0.3 mm, 0.7 mm and 1 mm. The electrodes were patterned by optical ultraviolet lithography, evaporation, and lift-off process. The permittivity distribution of BST film can be controlled by applying an external electro-static field between the electrodes.

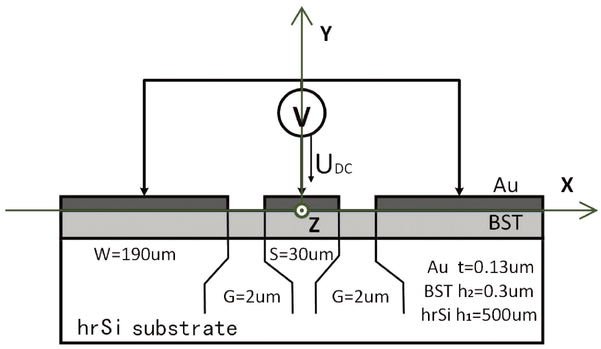

Fig. 1. Cross section of a coplanar waveguide (CPW).

2 Subregional Match 3-Dimensional finite element method

Following is the specific introduction of SM 3D FEM implementation.

2.1 Static electric field analysis

A 2D electrostatic field analysis method is used to accurately calculate the distribution of electric field strength in BST thin films. In this model, the

DOI: 10.1587/elex.13.20160713
Received July 20, 2016
Accepted August 22, 2016
Publicized September 23, 2016
Copyedited October 10, 2016

permittivity of the BST is a changeable parameter to see if the value of the permittivity have an impact on the electric field distribution. To validate the extraction of the electric field strength, the curves extracted using three distinct permittivity is compared in Fig. 2, exhibiting great agreement. Different permittivity has only a slight influence on electric field distribution, the relative difference $\Delta E = \max\left|\frac{E(\xi_{BST} = 200, X) - E(\xi_{BST} = 400, X)}{E(\xi_{BST} = 200, X)}\right|$ less than 1.4%.

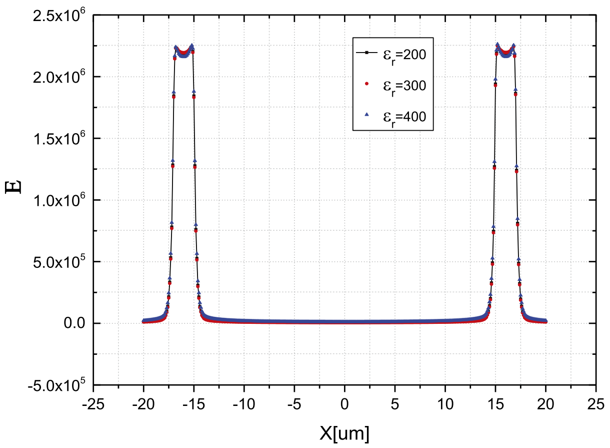

Fig. 2. Dependency of the electric field strength on the permittivity ξ_{BST} (Y = -0.15 um). The external voltage is U = 5 V.

In Fig. 3, graphs represent electric field strength E next to the slot area (12.5 um $\leq$ X $\leq$ 20 um), different curves representing electric field at different depths (different Y coordinates, see Fig. 1). Two high cusps of the electric field distribution exist close to the edges of the metal surface. The average DC-E-field distribution (averaging at different depths) show in illustration (a) in Fig. 3. We find the average DC-E-field distribution at two cusps area is the same as distribution at the middle of slot area. So fringing fields can be neglected, just as the uniform electric field distribution E = $\frac{U}{g}$ between two parallel plates with spacing d and the applied voltage U in slot area. Other areas seem have no electric field strength distribution (shown in Fig. 2). So as show in illustration (b) of Fig. 3, the relative permittivity of BST can be divided into two part (part A and part B), using constant permittivity in each part for simulation.

2.2 Three-dimensional (3D) finite element method (FEM)

3D FEM model is used to implement the permittivity extraction based on the S-parament-phase matching, narrowing the difference between measured and simulated S-parament-phase by adjusting permittivity in the SM 3D FEM model until the simulated S-parament-phase and the measured one are well matched, which means the difference between them is small enough. In order to extract BST films permittivity ξ_{BST}, we use conductivity of the metallization $\sigma = 32 \times 10^6$ S/m and permittivity of the hrSi substrate $\xi_{hrSi} = 11.7$ (implement using the same process [6, 7]) for simulation. Permittivity $\xi(f, E)$ dependent on frequency and electrical

DOI: 10.1587/elex.13.20160713
Received July 20, 2016
Accepted August 22, 2016
Publicized September 23, 2016
Copyedited October 10, 2016

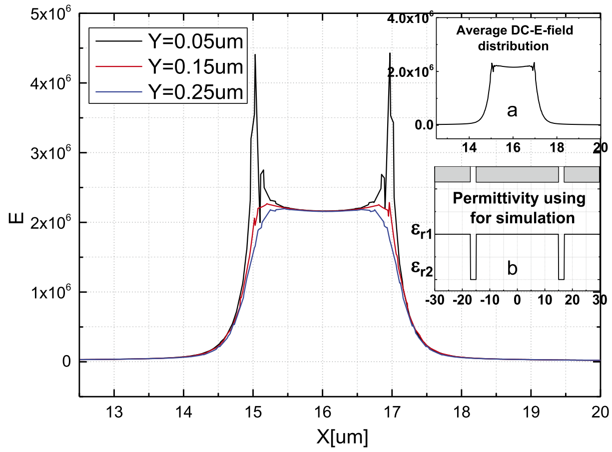

Fig. 3. Electric field strength distribution at different depths, a) average DC-E-field distribution in BST, b) permittivities using for simulation.

field strength is a changeable parameter. The SM 3D FEM model analyzing processes are repeated circularly. In each repeating cycle, ξ_{BST} is adjusted to a more accurate value. First, $\xi_1(f)$ (constant at each frequency) can be obtained due to 0 V-simulation (0 V external voltage). In this case $\xi_1(f) = \xi_2(f, 0\,\mathrm{V})$, permittivity and permeability are homogeneous in BST film, so $\xi_1(f)$ is easy obtained. Then, external DC voltage ($0\,\mathrm{V} \leq \mathrm{U} \leq 30\,\mathrm{V}$, $0\,\mathrm{V/um} \leq \mathrm{E} \leq 15\,\mathrm{V/um}$) is applied, result in the change of $\xi_2(f, E)$. This time $\xi_1(f)$ is a given number. Matching measured and simulated result circularly can extract permittivity $\xi_2(f, E)$ accurately.

Fig. 4 shows a typical mesh in SM 3D FEM model where about 1010668 area units, 161692 face units and 4466 side units are used to discretize the whole three-dimensional structure including the BST layer, the coplanar electrodes, the hrSi substrate and the ambient air. We focus on the corner metallization and the BST film where mesh surge in this area. The electrode is meshed with one layer of tetrahedron because of the skin effect. The skin depth is of 0.27 um at 110 GHz at an average conductivity of 32×10^6 S/m [6, 7], greater than thickness of the metal layer 0.13 um.

3 Experimental results

3.1 Permittivity extraction

The resulting permittivity range from 1 to 110 GHz is shown in Fig. 5. It is found that permittivity of BST thin films decrease over the measured frequency domain. Different color lines show the value of ξ_{BST} under different electric field strength. $\xi_{BST}(f, 0\,\mathrm{V})$ (black line) declines from 1148.9 to 311.7 smoothly when the frequency increases from 1 GHz to 110 GHz. Permittivity ξ_{BST} vs. electric field strength is shown in the inset picture of Fig. 5, permittivity at 100 GHz equals 315.8 at 0 V/um and reduces to 193.4 at 15 V/um.

DOI: 10.1587/elex.13.20160713
Received July 20, 2016
Accepted August 22, 2016
Publicized September 23, 2016
Copyedited October 10, 2016

IEICE Electronics Express, Vol.13, No.19, 1–7

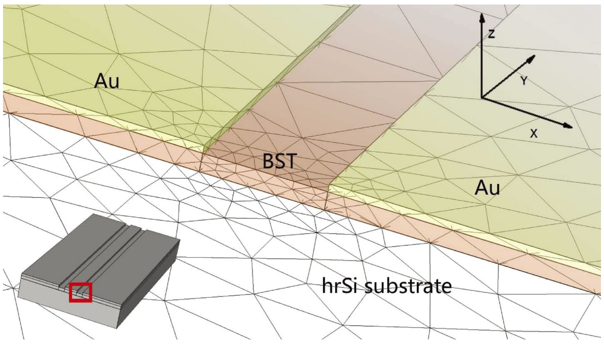

Fig. 4. Typical 3D mesh of the corner area of the central gold conductor.

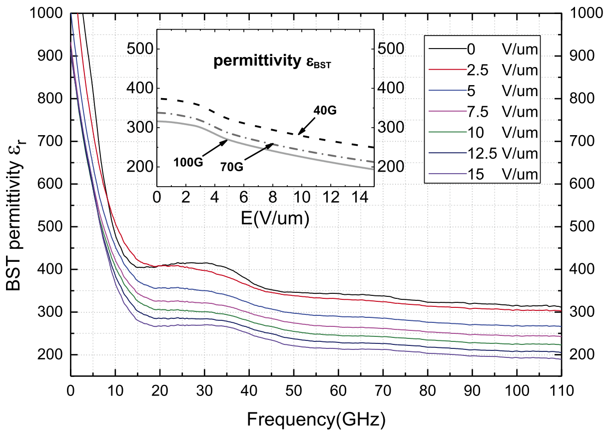

Fig. 5. Frequency behavior of the extracted ξ_{BST} and tuned ξ_{BST}.

3.2 Permittivity tunability

To validate the extraction of the field-dependent permittivity, the tunability $\Gamma_{\xi_{BST}}(f,E)$, defined as $\xi_{BST}(f,E) = \xi_{BST}(f,0)\cdot(1-\Gamma_{\xi_{BST}}(f,E))$, is shown in Fig. 6. $\xi_{BST}(f,0)$ is the untuned permittivity ($U_{dc}=0$) of the ferroelectric layer. Picture compared three distinct frequency tunability curves. The BST film tunability yields 33.2% (f = 40 GHz), 37.1% (f = 70 GHz) and 38.7% (f = 100 GHz) for the maximum applied electric tuning field-strength 15 V/um, exhibiting good consistency. In a wide frequency range (40 GHz to 100 GHz) the variation of the tunability $\Gamma_{\xi_{BST}}$ is relatively small.

Quadratic equation can be used according to Ref. 10. The tunability $\Gamma_{\xi_{BST}}(E)$ of the material can be modeled by a piecewise function.

$$\Gamma_{\xi_{BST}}(E) = \begin{cases} a_0 + a_1\cdot E + a_2\cdot E^2, & E\in(0,E_0] \\ b_0 + b_1\cdot E + b_2\cdot E^2, & E\in(E_0,15] \end{cases} \tag{1}$$

Parameters $E_0, a_0, a_1, a_2, b_0, b_1, b_2$ are calculated to fit curves (specific values shown in inset table in Fig. 6), exhibiting great agreement, less frequency dependency. Blue line is the average value,

$$\Gamma_{ave}(E) = \begin{cases} 0.0026667 - 0.0037679E + 0.0069549E^2, & E\in(0,4.7] \\ -0.010785 + 0.035728E - 0.00072459E^2, & E\in(4.7,15] \end{cases}$$

DOI: 10.1587/elex.13.20160713
Received July 20, 2016
Accepted August 22, 2016
Publicized September 23, 2016
Copyedited October 10, 2016

ELectronics EXpress

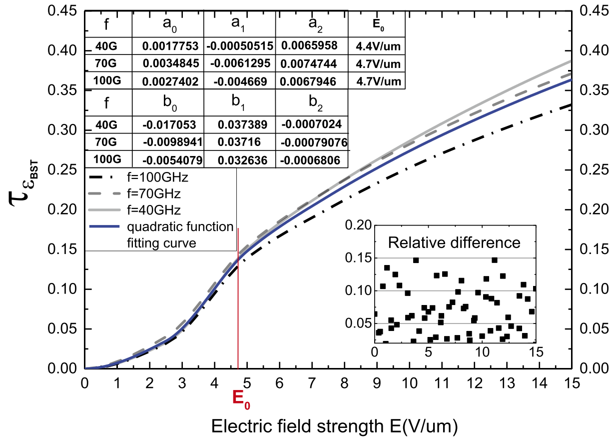

Fig. 6. Extracted tunability curves.

it can be used to represent BST film permittivity tunability within the frequency range from 40 GHz to 100 GHz. In order to describe the matching degree between Γ_{ave} and Γ_{meas}, the relative difference is defined as $\Delta\Gamma = \frac{|\Gamma_{ave} - \Gamma_{meas}|}{\Gamma_{meas}}$. Relative difference $\Delta\Gamma$ of BST permittivity is displayed in the inset of Fig. 6. It can be observed that $\Delta\Gamma < 0.16$ over the whole electric field-strength range. Compared to the reported tunability of BST films [10], this is at least comparable for the same tuning field-strength. For future discussion of the BST material application techniques, this is a promising result.

4 Conclusion

In summary, we propose a SM FEM model to extract the non-uniform permittivity of BST thin films. We apply the method to the $Ba_{0.5}Sr_{0.5}TiO_3$ film deposited directly onto the hrSi substrate. In order to obtained permittivity more precisely, we divided the BST film into several regions, and each area is evaluated separately. $\Gamma_{\xi_{BST}}$ is defined to describe the permittivity tunability. In our experiment, $\Gamma_{\xi_{BST}}$ is almost unchanged in a wide frequency domain, $\Delta\Gamma < 0.16$ over the whole electric field-strength range. The relative dielectric permittivity ξ_{BST} at 0 V equals 1148.9 at 1 GHz and reduces to 311.7 at 110 GHz, and ξ_{BST} at 100 GHz equals 315.8 at 0 V and declines to 193.4 at 30 V. The tunability of BST film is about 38.7%.

DOI: 10.1587/elex.13.20160713
Received July 20, 2016
Accepted August 22, 2016
Publicized September 23, 2016
Copyedited October 10, 2016